Biophysical Chemistry 161 (2012) 8–16

Contents lists available at SciVerse ScienceDirect

Biophysical Chemistry

journal homepage: http://www.elsevier.com/locate/biophyschem

Electric-field-enhanced nutrient consumption in dielectric biomaterials that contain anchorage-dependent cells ☆

Laurence A. Belfiore *,[1], Michael L. Floren [1], Carol J. Belfiore

Department of Chemical & Biological Engineering, Colorado State University, Fort Collins, CO 80523, USA

HIGHLIGHTS

- Reaction–diffusion equation is analyzed in electric-field-stimulated porous biomaterials.
- Critical intra-tissue Damköhler number is quantified in the presence of an electric potential.
- Damköhler and Deborah numbers quantify electric-field-stimulated chemical kinetics.
- Mass transfer boundary layer thickness depends on the Damköhler and Deborah numbers.

GRAPHICAL ABSTRACT

Schematic representation of cylindrical biomaterials in a dielectric-sandwich configuration subjected to harmonic electric potential differences across the capacitor plates, with radial diffusion of nutrients inward to support cell proliferation and sustainability.

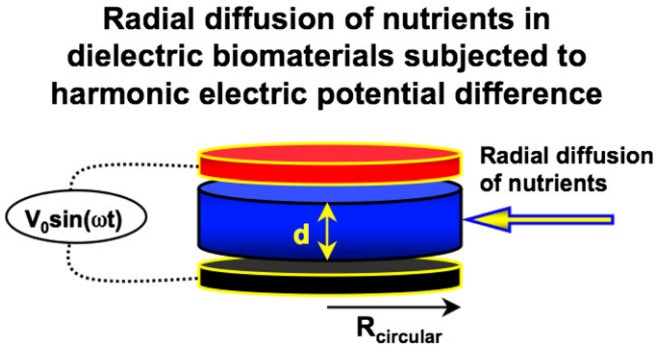

ARTICLE INFO

Article history:
Received 16 September 2011
Received in revised form 19 October 2011
Accepted 28 October 2011
Available online 10 November 2011

Keywords:
Fick's 2nd law
Unsteady state diffusion
Reaction–diffusion equation
Electric-field-enhanced diffusion
Intra-tissue diffusion
Viscoelastic biomaterial
Complex dielectric constant
Electric Damköhler number
Deborah number
von Kármán–Pohlhausen profile method
Mass transfer boundary layer thickness

ABSTRACT

This research contribution addresses electric-field stimulation of intra-tissue mass transfer and cell proliferation in viscoelastic biomaterials. The unsteady state reaction–diffusion equation is solved according to the von Kármán–Pohlhausen integral method of boundary layer analysis when nutrient consumption and tissue regeneration occur in response to harmonic electric potential differences across a parallel-plate capacitor in a *dielectric-sandwich* configuration. The partial differential mass balance with diffusion and electro-kinetic consumption contains the Damköhler (Λ^2) and Deborah (De) numbers. Zero-field and electric-field-sensitive Damköhler numbers affect nutrient boundary layer growth. Diagonal elements of the 2nd-rank diffusion tensor are enhanced in the presence of weak electric fields, in agreement with the formalism of equilibrium and nonequilibrium thermodynamics. Induced dipole polarization density within viscoelastic biomaterials is calculated via the real and imaginary components of the complex dielectric constant, according to the Debye equation, to quantify electro-kinetic stimulation. Rates of nutrient consumption under zero-field conditions are described by third-order kinetics that include local mass densities of nutrients, oxygen, and attached cells. Thinner nutrient boundary layers are stabilized at shorter dimensionless diffusion times when the zero-field intra-tissue Damköhler number increases above its initial-condition-sensitive critical value [i.e., $\{\Lambda^2_{\text{zero-field}}\}_{\text{critical}} \geq 53$, see Eq. (23)], such that the biomaterial core is starved of essential ingredients required for successful proliferation. When tissue regeneration occurs above the critical electric-field-sensitive

☆ This manuscript commemorates the 100th anniversary of the birth of Olivia DeVito Belfiore on June 18th, 1911, and the death of her mother upon childbirth. It is submitted in memory of the victims of the terrorist attacks 10 years ago in New York, Washington DC, and Shanksville Pennsylvania.

* Corresponding author.
E-mail address: belfiore@engr.colostate.edu (L.A. Belfiore).
[1] Presently at: Department of Materials Engineering & Industrial Technologies, University of Trento, via Mesiano 77, 38050 Trento, Italy.

0301-4622/$ – see front matter
doi:10.1016/j.bpc.2011.10.003

intra-tissue Damköhler number, the electro-kinetic contribution to nutrient consumption cannot be neglected. The critical electric-field-sensitive intra-tissue Damköhler number is proportional to the Deborah number.

1. Introduction

Biological effects associated with exposure to electric fields have been well-documented during the past 50 years on isolated cells [1] and tissues [2]. Cellular phenomena associated with proliferation, differentiation, and regeneration, such as wound healing [3], in the presence of electric fields have been studied extensively. Cellular activities, such as altered transcription [4], protein synthesis [5,6] and migratory patterns [7] can be influenced by electrical stimuli. Significant progress has occurred on the application of electric fields to treat a variety of bone disorders [8–11]. Upon exposure to electric fields, one side of the cell becomes hyperpolarized while the opposite side is depolarized [12]. Electric potential differences across biological membranes catalyze fundamental physiological processes, including ATP synthesis and growth [13]. Pulsed electromagnetic stimulation at 7.5 Hz reduces the loss of bone mass, enhances osteoblast proliferation, and accelerates DNA synthesis [12,14]. Hence, therapeutic treatments employing electric fields have been developed for bone disorders. It is well accepted that substrate surface charge significantly influences cell attachment [15,16]. Grafting various ionic and non-ionic moieties to polymer surfaces increases adhesion and proliferation of cells on positively charged substrates [17,18]. Bone cells modulate the activity of hormones, growth factors, and cytokines when exposed to electromagnetic stimuli, and electric fields promote osteogenesis [19]. In eukaryotic cells, external electric fields affect development, regeneration, and motility [13]. An increase in osteoblast proliferation occurs when rabbit bone marrow is electrically stimulated [20]. Encouraging results have been reported on neuronal stem cells in which adhesion, proliferation, and differentiation are facilitated by electrically conductive polymeric fibers [21]. Modulation frequency of the external electric potential also influences the activity of neuronal cell lines. Upon exposure to small-amplitude ac electric fields at a frequency of 1 Hz, murine neuronal stem cells encapsulated in alginate hydrogels exhibit improved viability by approximately 1 order of magnitude [22]. This excitation frequency is employed in numerical simulations to stimulate tissue regeneration in dielectric biomaterials, without introducing a time-average of the electric potential. Dynamic models with the potential to predict macroscale behavior from the microscale continuum are useful to describe underlying multi-scale processes that occur when tissue regeneration is stimulated by an electric potential.

2. Induced dipole polarization in dielectric solids subjected to harmonic electric potential difference

The dipole polarization vector in dielectric biomaterials, with dimensions of Coulomb-cm, is defined by the ensemble average of microscopic dipole moments [23]. When dielectrics are polarized in the presence of an electric field, the dipole polarization vector is nonzero. For isotropic dielectrics that respond linearly to external fields, the dipole polarization vector is parallel to the electric field everywhere within the material [24], with a scalar proportionality constant known as the polarization coefficient or the dielectric susceptibility, $\kappa = (\varepsilon - \varepsilon_0)$ Volume$/4\pi$, where ε is the dielectric permeability and ε_0 is the permittivity of free space (i.e., 8.854×10^{-12} C^2/[N-m^2]). Consider spherically shaped mammalian cells that consume nutrients and grow axisymmetrically in the absence of external fields, natural fluctuations, and their own motility on biocompatible surfaces. When the surface is polarized, the intracellular medium experiences induced polarization that perturbs axisymmetric growth [13], analogous to the *symmetry-breaking phenomenon* that generates mechanical stress imbalance on the cell's outer "comet-shaped" surface [25]. It is postulated that dipole polarization in dielectric biomaterials catalyzes rates of nutrient consumption by anchorage-dependent cells. Hence, kinetic models are developed that contain an electric-field-sensitive contribution, based on analysis of the Debye equation [i.e., Eq. (1)] for a single relaxation process characterized by one viscoelastic time constant λ (T) when dielectric materials contain no excess charge carriers [26]. The electrical analog of the Voigt model, with $\lambda = RC$, contains resistive R and capacitive C elements in series, such that the voltage drops are additive and the total dipole polarization is given by the product of the dielectric susceptibility κ with the external electric field E. This is equivalent to defining the effective field as a sum of the external field and an internal contribution that scales linearly with polarization density. Hence, dipole polarization density P (t), with dimensions of Coulomb-cm/cm^3, is calculated in the presence of an external ac electric field E (t;ω) according to [26,27];

$$\frac{dP}{dt} + \frac{1}{\lambda(T)}P = \varepsilon_0\{\varepsilon_S - \varepsilon_\infty\}\frac{1}{\lambda(T)}E(t;\omega)$$
$$P(t \Rightarrow -\infty) = 0 \tag{1}$$

where λ (T) is a temperature-dependent dipole relaxation time of the viscoelastic biomaterial, and ε_S and ε_∞ are the static and high-frequency (i.e., optical) dielectric constants of the material, respectively. The dipolar relaxation strength is $\varepsilon_S - \varepsilon_\infty$. Under isothermal conditions, in which λ, ε_S, and ε_∞ are constant, solution of Eq. (1) is obtained via application of the integrating factor method for first-order inhomogeneous ODEs;

$$P(t;\omega) = \frac{\varepsilon_0\{\varepsilon_S - \varepsilon_\infty\}}{\lambda}\exp\left\{\frac{-t}{\lambda}\right\}\int_{t'\Rightarrow-\infty}^{t} E\left(t';\omega\right)\exp\left\{\frac{t'}{\lambda}\right\}dt' \tag{2}$$

If the harmonic electric potential difference applied across the capacitor plates in a *dielectric sandwich* configuration is given by;

$$V(t;\omega) = V_0\sin(\omega t) \tag{3}$$

then the external ac electric field is $E(t;\omega) = V(t;\omega)/d$, where d is the spacing between the plates. The induced dipole polarization in dielectric biomaterials exhibits time and frequency dependence according to Eq. (4). No attempt is made to connect biomaterial polarization to intracellular polarization. Hence, dielectric properties of the biocompatible matrix influence stimulated nutrient consumption in the presence of an electric potential;

$$P(t;\omega) = \frac{\varepsilon_0\{\varepsilon_S - \varepsilon_\infty\}}{\lambda}\frac{V_0}{d}\exp\left\{\frac{-t}{\lambda}\right\}\int_{t'\Rightarrow-\infty}^{t'=t}\exp\left\{\frac{t'}{\lambda}\right\}\sin\left(\omega t'\right)dt' \tag{4}$$
$$= \frac{\varepsilon_0\{\varepsilon_S - \varepsilon_\infty\}}{\lambda}\frac{V_0}{d}\frac{\omega\lambda^2}{1+\omega^2\lambda^2}\left\{\frac{1}{\omega\lambda}\sin(\omega t) - \cos(\omega t)\right\}$$
$$= \varepsilon_0\frac{V_0}{d}\left\{\varepsilon'(\omega)\sin(\omega t) - \varepsilon''(\omega)\cos(\omega t)\right\}$$
$$\varepsilon'(\omega) = \{\varepsilon_S - \varepsilon_\infty\}\frac{1}{1+\omega^2\lambda^2} = \{\varepsilon_S - \varepsilon_\infty\}\frac{1}{1+De^2}$$
$$\varepsilon''(\omega) = \{\varepsilon_S - \varepsilon_\infty\}\frac{\omega\lambda}{1+\omega^2\lambda^2} = \{\varepsilon_S - \varepsilon_\infty\}\frac{De}{1+De^2}$$

The scaling of time in viscoelasticity (i.e., material response time λ relative to a characteristic experimental timescale, $1/\omega$) is accomplished

via the Deborah number De, which is given by $\omega\lambda$ (T) for a one-time-constant model [28]. For a Maxwell-like RC-circuit (i.e., with R and C in parallel, and $\lambda = RC$), time-dependent polarization in the capacitive element which stores electrical energy without power dissipation, is completely *in-phase* with the oscillatory electric potential difference V and contains the real part $\varepsilon'(\omega)$ of the complex dielectric constant: $\varepsilon^* = \varepsilon'(\omega) - j\varepsilon''(\omega)$, where $j = \sqrt{(-1)}$. Electrical energy dissipation occurs in the resistive branch, where current and voltage drop are in-phase, but polarization or charge density is completely *out-of-phase* with V and contains the imaginary part $\varepsilon''(\omega)$ of the complex dielectric constant. Eq. (4) for the induced dipole polarization density exhibits the same functional form if the actual dielectric biomaterial requires a distribution of dipole relaxation times. However, the real and imaginary components of the complex dielectric constant, $\varepsilon'(\omega)$ and $\varepsilon''(\omega)$, contain additional terms similar to those in Eq. (4) for each significant relaxation time. If distributed relaxation processes are operative in cells and tissues, then fractional calculus [29] might be useful to describe input–output behavior of biological systems, due to the fractal or porous structure of the components. Fractional-order complex impedance in circuit models allows one to describe transient and steady state frequency response of dielectrics, biological tissue, bio-electrodes, and electrode/cardiac-tissue interfaces in pacemaker electrodes with diffusion-limited electrochemical reactions at the electrode surface [29].

3. Electric-field-enhanced rates of nutrient consumption in dielectric biomaterials

It is necessary to consider electro-kinetic coupling between the induced dipole polarization density in Eq. (4) and nutrient consumption when cells anchored to dielectric biomaterials respond to an electric potential difference across the capacitor plates. This is the electrical analog of stress–kinetic scalar cross-phenomena when the state of deformation in viscoelastic biomaterials is transmitted to anchorage-dependent cells, and harmonic excitation catalyzes enhanced rates of nutrient consumption via *symmetry breaking* [25], as mentioned above. In light of the fact that the potential bias of gold electrodes affects elongated growth of *Pseudomonas fluorescens* cells [13], a modification of root-mean-square dipole polarization density that does not average dependence on time is employed in Eq. (5) to quantify pseudo-homogeneous rates of nutrient consumption. In the spirit of *linear cross-couplings;*

$$R_{\substack{\text{homogeneous}\\ \text{nutrient}\\ \text{consumption}}} = k_{\text{zero-field}}\rho_{\text{nutrient}}\rho_{\text{oxygen}}\rho_{\text{cells}} + \gamma_{\text{electric}}\sqrt{P^2(t;\omega)}$$
$$P(t;\omega) = \varepsilon_0\frac{V_0}{d}\left\{\varepsilon'(\omega)\sin(\omega t) - \varepsilon''(\omega)\cos(\omega t)\right\} \quad (5)$$

where the scalar electro-kinetic coupling coefficient γ_{electric} has dimensions of nutrient mass per thickness of the viscoelastic biomaterial per Coulomb-time. Electro-kinetic coupling via the second term on the right side of Eq. (5) represents a zeroth-order rate of nutrient consumption. Zero-field rates of nutrient consumption, given by the first term on the right side of Eq. (5), require the presence of nutrients, oxygen, and attached cells whose receptors form complexes with functional groups in the chemical structure of conformationally accessible proteins dispersed throughout, or embedded within, porous biomaterials. Both kinetic rate coefficients in Eq. (5), $k_{\text{zero-field}}$ and γ_{electric}, depend on the protein's folding characteristics in a thin aqueous film on the interior biomaterial surface. Hence, the appropriate signaling exists for cells to consume nutrients and proliferate within the context of regenerative medicine.

4. Stoichiometric requirements for nutrient consumption by anchorage-dependent mammalian cells

This application of tissue regeneration in dielectric biomaterials includes zero-field and electro-kinetic rates of nutrient consumption, where the latter is stimulated by a harmonic electric potential applied across capacitor plates. It is necessary to connect the rate of nutrient consumption to the rate of cell proliferation. Effective biomass yields between 40% and 50% have been reported for a selected group of glucose-fed micro-organisms [30,31]. Hence, $\sigma_{\text{cells}}/\sigma_{\text{nutrient}} \approx 0.45$ is employed in Eq. (6), in consideration of the fact that some nutrient consumption could be channeled into other products and metabolic activities not related to cell proliferation, such as energetic support for cell mobility and sustainability. Yield coefficients that characterize cell mass produced per mass of oxygen consumed (i.e., $\sigma_{\text{cells}}/\sigma_{\text{oxygen}} \approx 0.45$) for the production of hematopoietic cells in 3-dimensional perfusion bioreactors suggest a 1:1 mass ratio for oxygen to nutrient consumption [32,33]. Both of these stoichiometric ratios (i.e., $\sigma_{\text{cells}}/\sigma_{\text{nutrient}} \approx 0.45$ and $\sigma_{\text{oxygen}}/\sigma_{\text{nutrient}} \approx 1$) are required to simulate tissue regeneration via the following relations between mass densities for nutrients, ρ_{nutrient}, and species *i*, ρ_i, in porous biomaterials;

$$\rho_i(x,t) - \rho_i(x = L, t = 0) = \upsilon_i\frac{\sigma_i}{\sigma_{\text{nutrient}}}\{\rho_{\text{nutrient}}(x = L, t = 0) - \rho_{\text{nutrient}}(x,t)\} \quad (6)$$

where $\upsilon_{\text{cells}} = +1$, and $\upsilon_{\text{oxygen}} = -1$. These parameters are used in Eqs. (19), (22) and (23).

5. Modified diffusion equation for electric-field-enhanced nutrient consumption in cylindrical biomaterials

Fick's second law of diffusion with nutrient consumption (i.e., the *modified diffusion equation*) describes the transient and spatial dependence of the mass density of each reactive species (i.e., nutrients, oxygen, growth factors, etc.) within a dielectric biomaterial of radius R_{circular} and thickness d that supports tissue regeneration [34–37]. In reference to Fig. 1, with one-directional flux radially inward (i.e., transverse to the electric-field direction), one must solve the reaction–diffusion equation [38] for nutrient mass density, ρ_{nutrient} (r,t);

$$\frac{\partial\rho_{\text{nutrient}}}{\partial t} = D_{\text{A,effective,intra-tissue}}\frac{1}{r}\frac{\partial}{\partial r}\left\{r\frac{\partial\rho_{\text{nutrient}}}{\partial r}\right\} - R_{\substack{\text{homogeneous}\\ \text{nutrient}\\ \text{consumption}}} \quad (7)$$

where time t accounts for transient response, and $D_{\text{A,effective,intra-tissue}}$ is the electric-field-enhanced effective diffusion coefficient of species A within the porous matrix. The total pseudo-homogeneous rate of nutrient consumption by anchorage-dependent cells is calculated via Eq. (5) in the presence and absence of electric-field stimulation. The thermodynamics of irreversible processes yields the following equation for ordinary molecular diffusion coefficients [39] in binary mixtures, D_{AB};

$$\rho D_{AB} \approx \left\{\frac{\partial}{\partial\omega_A}\left[\frac{\mu_A}{MW_A} - \frac{\mu_B}{MW_B}\right]\right\}_{T,p} \approx \left[\frac{1}{MW_A} + \frac{x_A}{x_B MW_B}\right]\left\{\frac{\partial\mu_A}{\partial\omega_A}\right\}_{T,p} \quad (8)$$

where ρ is overall mass density, μ is chemical potential, x is mole fraction, and ω_A is mass fraction. In the weak-field limit, when systems do not achieve electric saturation, the electric field dependence of species chemical potentials [28] is written in terms of partial molar dielectric susceptibilities, κ_A;

$$\mu_A(T,p,E,\text{composition}) = \{\mu_A(T,p,\text{composition})\}_{\text{zero-field}} - \frac{1}{2}E^2\kappa_A + \ldots \quad (9)$$

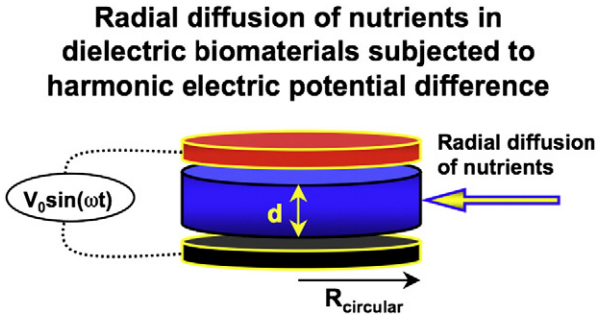

Fig. 1. Schematic representation of cylindrical biomaterials in a dielectric-sandwich configuration subjected to harmonic electric potential differences across the capacitor plates, with radial diffusion of nutrients inward to support cell proliferation and sustainability.

Hence, effective intra-tissue diffusivities $D_{A,effective,intra-tissue}$ in the presence of weak electric fields include (i) a zeroth-field Einstein-like expression (i.e., $D=\chi k_{Boltzmann}T$, $\chi=$ mobility), that scales inversely with molar mass and is reduced in magnitude by the porosity and tortuosity of the biomaterial matrix [39], and (ii) a quadratic enhancement [40] that scales as E^2;

$$D_{A,effective,intra-tissue}=\frac{\varepsilon_{porosity}}{\tau_{tortuosity}}\chi k_{Boltzmann}T\left\{1+\Omega E^2+\ldots\right\}=D_{A,zero-field}\left\{1+\Omega E^2+\ldots\right\} \quad (10)$$

In Eq. (10), χ is the inverse of a friction coefficient (i.e., mobility) and Ω is a positive constant that scales linearly with the compositional dependence of the partial molar dielectric susceptibility of the diffusing species. However, a detailed analysis of quantum diffusion in semiconductors [41,42] reveals that one of the diagonal elements of the diffusion tensor exhibits a $1/E^2$ dependence on field strength. The dielectric-sandwich configuration is illustrated in Fig. 1, with radial diffusion unaffected by electric field vectors oriented in the z-direction.

Pulsed electric-field-enhanced interstitial transport of plasmid DNA has been investigated *in vivo* in tumors, revealing that the presence of the field might be critical for diffusion of pDNA from interstitial space to transient pores in the plasma membrane of electro-permeabilized cells [43]. Due to the impermeable capacitor plate boundaries, the circumference of the regenerative matrix (i.e., $r=R_{circular}$) is exposed to dissolved oxygen in the well-mixed nutrient medium at time $t=0$, allowing radial diffusion of essential ingredients inward to support sustainability and proliferation of anchorage-dependent cells that are seeded uniformly in a porous matrix. The required boundary conditions are;

$$\begin{aligned}&\rho_{nutrient}=\rho_{nutrient,medium};\ r=R_{circular};\ t>0\\&\frac{\partial\rho_{nutrient}}{\partial r}=0;\ \text{and}\ \rho_{nutrient}\Rightarrow 0;\ r=r_{critical}(t)\\&\rho_{nutrient}=0;\ t=0;\ r_{critical}\le r<R_{circular}\end{aligned} \quad (11)$$

The zero-flux and zero-mass–density boundary condition at $r_{critical}$ is reminiscent of a boundary-layer problem because the central core is nutrient-starved at short times for all reasonable values of the intra-tissue Damköhler number. Dimensionless variables are introduced for nutrient mass density, spatial position in the radial direction, and time, where $\Theta_{Diffusion,zero-field}=R^2_{circular}/D_{A,zero-field}$ represents a characteristic time constant for intra-tissue diffusion under zero-field conditions [39].

$$\begin{aligned}&\text{Nutrient mass density; } \Psi_A=\frac{\rho_{nutrient}}{\rho_{nutrient,medium}}\\&\text{Spatial coordinate in the radial direction; } \eta=\frac{r}{R_{circular}}\\&\text{Dimensionless diffusion time; } \tau=\frac{tD_{A,zero-field}}{R^2_{circular}}=\frac{t}{\Theta_{Diffusion,zero-field}}\end{aligned} \quad (12)$$

This allows one to re-express the modified diffusion equation and its boundary conditions in dimensionless form for nutrient mass density $\Psi_A(\eta,\tau)$;

$$\begin{aligned}&\frac{\partial\Psi_A}{\partial\tau}=\left(1+\Omega E^2\right)\left\{\frac{\partial^2\Psi_A}{\partial\eta^2}+\frac{1}{\eta}\frac{\partial\Psi_A}{\partial\eta}\right\}-\Lambda^2_{A,zero-field}\Psi_A\Psi_{oxygen}\Psi_{cells}\\&\qquad-\frac{\Lambda^2_{A,electric}}{1+De^2}\sqrt{\{\sin(\omega t)-De\cos(\omega t)\}^2}\\&\Psi_A=1;\ \eta=1;\ \tau>0\\&\frac{\partial\Psi_A}{\partial\eta}=0;\ \text{and}\ \Psi_A\Rightarrow 0;\ \eta=1-\delta_{MTBLT}(\tau)\\&\Psi_A=0;\ \tau=0;\ 1-\delta_{MTBLT}(\tau)\le\eta<1\\&E(t;\omega)=\frac{V_0}{d}\sin(\omega t)\\&1+\Omega E^2=1+\xi\Lambda^4_{A,electric}\sin^2(\omega t)\\&De=\omega\lambda(T);\ \omega t=De\frac{\Theta_{Diffusion,zero-field}}{\lambda(T)}\tau\end{aligned} \quad (13)$$

$\Lambda^2_{A,zero-field}$ is the species-specific zero-field intra-tissue Damköhler number that represents an order-of-magnitude ratio of the consumption rate to the rate of diffusion toward anchorage-dependent cells [34,39], when both rate processes occur under zero-field conditions. Hence:

$$\Lambda^2_{A,zero-field}=k_{zero-field}\rho^2_{nutrient,medium}\Theta_{Diffusion,zero-field} \quad (14)$$

where $\rho_{nutrient,medium}$ is the mass density of nutrients in the vicinity of the external tissue circumference, and $k_{zero-field}$ is the pseudo-volumetric third-order kinetic rate constant for nutrient consumption under zero-field conditions. The electric-field-sensitive intra-tissue Damköhler number is defined as the zeroth-order rate of nutrient consumption in the presence of an external electric field relative to the zero-field rate of intra-tissue diffusion toward anchorage-dependent cells:

$$\Lambda^2_{A,electric}=\frac{V_0}{d}\frac{\gamma_{electric}\varepsilon_0\{\varepsilon_S-\varepsilon_\infty\}}{\rho_{nutrient,medium}}\Theta_{Diffusion,zero-field} \quad (15)$$

where $\gamma_{electric}$ is the scalar electro-kinetic coupling coefficient, V_0 is the amplitude of the harmonic electric potential difference across the capacitor plates with gap thickness d, and $\varepsilon_S-\varepsilon_\infty$ is the dipolar relaxation strength of the viscoelastic biomaterial, or the difference between the static and high-frequency (i.e., optical) dielectric constants. Eq. (13) represents a unique example in the refereed journal literature where the Damköhler and Deborah numbers appear together in the reaction–diffusion equation to parameterize mass transfer in viscoelastic biomaterials [44] subjected to electric-field stimulation. The electric-field-sensitive intra-tissue Damköhler number [i.e., see Eq. (15)] is defined for the first time in this investigation. The concept of the intra-tissue Damköhler number in biological systems is analogous to the intrapellet Damköhler number for heterogeneous catalysis in packed reactors [38,39]. Electric field effects in complex cellular systems have been analyzed in two- and three-dimensions by (i) constructing *transport lattice*

networks that include nearest neighbor interactions and (ii) solving electric-circuit-law equations at nodes and around various closed loops [45]. A two-dimensional representation of the transient reaction–diffusion equation in spherical coordinates, with dependence on r and the polar angle, has been solved by the alternating-direction-implicit finite-difference algorithm in the presence of a first-order "sink" term where the kinetic rate constant is modified by a dc electric field, but the diffusion coefficient is parameterized under zero-field conditions [46]. Numerical solution of Eq. (13) via finite-difference calculus is awkward, due to the zeroth-order electric-field-sensitive rate of nutrient consumption that must be extinguished in the tissue's central core at short times when nutrients have not diffused inward to a significant extent. There are very few literature references that invoke the von Kármán–Pohlhausen *profile* method and solve the modified diffusion equation with chemical reaction [37,44] to predict transient mass transfer boundary layer thicknesses (i.e., 4 matches in Web of Science™ to *diffusion, reaction, von Kármán*). Profile methods have not been employed to solve mass transfer boundary layer problems in the presence of electro-kinetic stimulation.

6. Solution of the unsteady state reaction–diffusion equation according to the von Kármán–Pohlhausen integral method of boundary layer analysis

Several nonlinear reaction–diffusion equations, including Fisher's equation for transient 1-dimensional diffusion and 2nd-order growth, are discussed in reference [47]. Bendahmane and Karlsen [48] prove existence and uniqueness for a class of reaction–diffusion equations that simulate electro-physiological waves in cardiac tissue. Sherratt et al. [49] have analyzed solutions of the reaction–diffusion equation that include cell–cell and cell–matrix adhesion, random cell movement, and cell proliferation. In this investigation, the transient reaction–diffusion equation, given by Eq. (13), was solved for dimensionless nutrient mass density, $\Psi_A(\varphi)$, and the dimensionless mass transfer boundary layer thickness $\delta_{MTBLT}(\tau; \Lambda_{A,zero\text{-}field}, \Lambda_{A,electric})$ by postulating a quadratic function of the combined variable φ according to the von Kármán–Pohlhausen profile method of boundary layer analysis [37];

$$\Psi_A(\eta,\tau) = \Psi_A(\varphi) = \alpha + \beta\varphi + \zeta\varphi^2$$
$$\varphi = \frac{1-\eta}{\delta_{MTBLT}\left(\tau; \Lambda_{A,zero-field}, \Lambda_{A,electric}\right)} \tag{16}$$

The proposed quadratic function for dimensionless nutrient mass density Ψ_A in Eq. (16) is consistent with steady state profiles for zeroth-order rates of consumption in tissue with rectangular symmetry [37,39], for all values of both intra-tissue Damköhler numbers. Boundary conditions at $\eta=1$ [i.e., $\Psi_A(\varphi=0)=1$] and $\eta=1-\delta_{MTBLT}$ [i.e., $\{\partial\Psi_A/\partial\eta\}_{\varphi=1}=\Psi_A(\varphi=1)=0$] yield numerical values for the constants α, β, and ζ. Hence;

$$\Psi_A(\varphi=0)=\alpha=1$$
$$\Psi_A(\varphi=1)=\alpha+\beta+\zeta=0$$
$$\left\{\frac{\partial\Psi_A}{\partial\eta}\right\}_{\eta=1-\delta_{MTBLT}} = \frac{-1}{\delta_{MTBLT}\left(\tau; \Lambda_{A,zero-field}, \Lambda_{A,electric}\right)}\left\{\frac{\partial\Psi_A}{\partial\varphi}\right\}_{\varphi=1} \tag{17}$$
$$= \frac{-\beta-2\zeta}{\delta_{MTBLT}\left(\tau; \Lambda_{A,zero-field}, \Lambda_{A,electric}\right)} = 0$$

with $\alpha=1$, $\beta=-2$, $\zeta=1$. If $\Psi_A \Rightarrow 0$ with zero slope at $\varphi=1$, then the initial condition is satisfied as $\varphi \Rightarrow \infty$. Upon substitution of the postulated profile for $\Psi_A(\varphi)$ via Eq. (16) into Eq. (13), multiplication by δ_{MTBLT}, and integration with respect to φ from 0 to 1;

$$(1)\ \left\{\frac{\partial\Psi_A}{\partial\tau}\right\}_\eta = \frac{d\Psi_A}{d\varphi}\left\{\frac{\partial\varphi}{\partial\delta_{MTBLT}}\right\}_\eta \frac{d\delta_{MTBLT}}{d\tau} = \frac{-\varphi}{\delta_{MTBLT}}\{\beta+2\zeta\varphi\}\frac{d\delta_{MTBLT}}{d\tau}$$
$$(2) -\frac{d\delta_{MTBLT}}{d\tau}\int_0^1 \varphi\{\beta+2\zeta\varphi\}d\varphi = -\left\{\frac{1}{2}\beta+\frac{2}{3}\zeta\right\}\frac{d\delta_{MTBLT}}{d\tau}$$
$$(3)\ \left\{\frac{\partial^2\Psi_A}{\partial\eta^2}\right\}_\tau = \frac{1}{\delta_{MTBLT}^2}\frac{d^2\Psi_A}{d\varphi^2} = \frac{2\zeta}{\delta_{MTBLT}^2}$$
$$(4)\ \frac{1}{\eta}\left\{\frac{\partial\Psi_A}{\partial\eta}\right\}_\tau \underset{\zeta=1}{\overset{\beta=-2}{\Rightarrow}} \frac{2}{\delta_{MTBLT}}\int_0^1 \frac{1-\varphi}{1-\varphi\delta_{MTBLT}}d\varphi = \frac{2}{\delta_{MTBLT}}\left\{\frac{\delta_{MTBLT}+(1-\delta_{MTBLT})\ln[1-\delta_{MTBLT}]}{\delta_{MTBLT}^2}\right\} \tag{18}$$

one obtains a first-order ordinary differential equation (ODE) for $\delta_{MTBLT}(\tau; \Lambda_{A,zero\text{-}field}, \Lambda_{A,electric})$ that represents conservation of nutrient mass over the thickness of the boundary layer;

$$\frac{1}{3}\frac{d\delta_{MTBLT}}{d\tau} = \left\{1+\xi\Lambda_{A,electric}^4\sin^2(\omega t)\right\}\left[\frac{4}{\delta_{MTBLT}}+\frac{2}{\delta_{MTBLT}^2}(1-\delta_{MTBLT})\ln\{1-\delta_{MTBLT}\}\right]$$
$$-\frac{\delta_{MTBLT}\Lambda_{A,electric}^2}{1+De^2}\sqrt{\{\sin(\omega t)-De\cos(\omega t)\}^2}$$
$$-\delta_{MTBLT}\Lambda_{A,zero-field}^2\int_{\varphi=0}^1 \Psi_A(\varphi)\Psi_{oxygen}(\varphi)\Psi_{cells}(\varphi)d\varphi \tag{19}$$

The differential equation for δ_{MTBLT} in Eq. (19) reduces to Eq. (20) at steady state in the absence of electrical stimuli (i.e., $\Lambda_{A,electric} \Rightarrow 0$) when the dimensionless nutrient mass transfer boundary layer thickness is independent of dimensionless diffusion time τ.

$$\delta_{MTBLT}^2\Lambda_{A,zero-field}^2\int_{\varphi=0}^1 \Psi_A(\varphi)\Psi_{oxygen}(\varphi)\Psi_{cells}(\varphi)d\varphi - \frac{2}{\delta_{MTBLT}}(1-\delta_{MTBLT})\ln\{1-\delta_{MTBLT}\} = 4 \tag{20}$$

For zeroth-order nutrient consumption in the absence of electric fields, the integral on the left side of Eq. (20) is unity and the steady-state dimensionless nutrient boundary layer thickness in long cylindrical biomaterials depends on the zero-field intra-tissue Damköhler number according to Eq. (21);

$$\delta_{MTBLT}^2\Lambda_{A,zero-field}^2 - \frac{2}{\delta_{MTBLT}}(1-\delta_{MTBLT})\ln\{1-\delta_{MTBLT}\} = 4 \tag{21}$$

This is consistent with a critical zero-field intra-tissue Damköhler number, $\{\Lambda_{A,zero\text{-}field}\}=2$, in cylindrical biomaterials [37,39] when $\delta_{MTBLT}=1$, because the second term on the left side of Eq. (21) vanishes according to l'Hopital's rule. When $\Lambda_{A,zero\text{-}field}>2$ for zeroth-order kinetics in porous tissue with cylindrical symmetry, $\delta_{MTBLT}<1$ and the central core is starved of essential ingredients required for cell proliferation at steady state, according to the lower curve in Fig. 2.

When zero-field consumption by anchorage-dependent cells follows 3rd-order kinetics, requiring the presence of several ingredients as described by Eqs. (5) and (20), reasonable conditions at the

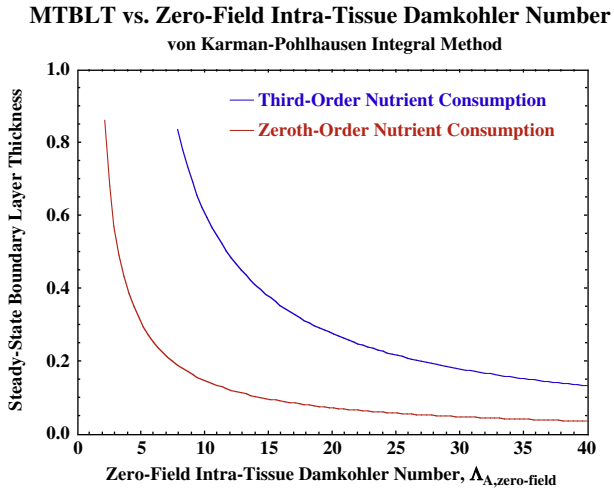

Fig. 2. Effect of the intra-tissue Damköhler number $\Lambda_{A,zero\text{-}field}$ on the steady-state dimensionless nutrient boundary layer thickness δ_{MTBLT} in cylindrical biomaterials under zero-field conditions. *Upper curve:* calculations are based on Eqs. (20) and (22) when nutrient consumption follows complex third-order kinetics, and the initial condition for cellular and oxygen mass densities on the external biomaterial surface are: $\Psi_{cells}\ (\eta=1,\tau=0)=0.25$ and $\Psi_{oxygen}\ (\eta=1,\tau=0)=1$, such that $\delta_{MTBLT}=1$ when $\{\Lambda_{A,zero\text{-}field}\}_{critical}=\sqrt{(53)}$. *Lower curve:* calculations are based on Eq. (21) for zeroth-order nutrient consumption, such that $\delta_{MTBLT}=1$ when $\{\Lambda_{A,zero\text{-}field}\}_{critical}=2$. von Karman–Pohlhausen predictions from Eq. (21) for zeroth-order kinetics are essentially indistinguishable from the exact solution obtained via the following equation based on steady-state analysis [37,39]; $2\delta_{MTBLT}-\delta_{MTBLT}^2+2(1-\delta_{MTBLT})^2\ln\{1-\delta_{MTBLT}\}=\frac{4}{\Lambda^2_{A,zero-field}}$.

biomaterial/nutrient-medium interface (i.e., $r=R_{circular}$) yield the following tissue-averaged dimensionless rate of consumption:

$$\Psi_A(\varphi)=\frac{\rho_{nutrient}}{\rho_{nutrient,medium}}=\alpha+\beta\varphi+\zeta\varphi^2$$

$$\Psi_i(\varphi)-\frac{\rho_i(r=R_{circular},t=0)}{\rho_{nutrient,medium}}=\upsilon_i\frac{\sigma_i}{\sigma_{nutrient}}\{1-\Psi_A(\varphi)\};\ i=\text{cells, oxygen}$$

$$\int_{\varphi=0}^{1}\Psi_A(\varphi)\Psi_{oxygen}(\varphi)\Psi_{cells}(\varphi)d\varphi$$

$$\underset{\Psi_{cells}(\eta=1,\tau=0)=0.25}{=}\begin{Bmatrix}-0.0343+0.06\Psi_{oxygen}(\eta=1,\tau=0)-0.133\Psi_{cells}\\ \times(\eta=1,\tau=0)+0.333\Psi_{oxygen}(\eta=1,\tau=0)\Psi_{cells}\\ \times(\eta=1,\tau=0)\\ \approx 0.040\ \left[\text{when}\Psi_{oxygen}(\eta=1,\tau=0)=0.75\right]\\ \approx 0.076\ \left[\text{when}\Psi_{oxygen}(\eta=1,\tau=0)=1\right]\end{Bmatrix} \tag{22}$$

Now, cylindrical biomaterials can operate further into the diffusion-limited regime at steady state, before regeneration ceases in the tissue's central core (Fig. 2, upper curve), because the initial-condition-sensitive critical zero-field intra-tissue Damköhler number is evaluated via Eqs. (20) and (22) when $\delta_{MTBLT}=1$. This calculation is provided in Eq. (23). In the presence of convection, diffusion, and zeroth-order nutrient consumption, similar criteria have been developed to avoid starvation in the central core of porous biological pellets with spherical symmetry [50].

$$\left\{\Lambda^2_{A,zero-field}\right\}_{critical}=\frac{4}{\int_{\varphi=0}^{1}\Psi_A(\varphi)\Psi_{oxygen}(\varphi)\Psi_{cells}(\varphi)d\varphi}$$

$$\underset{\Psi_{cells}(\eta=1,\tau=0)=0.25}{=}\begin{Bmatrix}\approx\frac{4}{0.040}=100\ \left[\text{when}\Psi_{oxygen}(\eta=1,\tau=0)=0.75\right]\\ \approx\frac{4}{0.076}\approx 53\ \left[\text{when}\Psi_{oxygen}(\eta=1,\tau=0)=1\right]\end{Bmatrix} \tag{23}$$

7. Parametric analysis of electric-field-sensitive nutrient consumption in dielectric biomaterials

The time-dependent ODE in Eq. (19) was solved for the development of $\delta_{MTBLT}(\tau;\Lambda_{A,zero\text{-}field},\Lambda_{A,electric})$, subject to the initial condition $\delta_{MTBLT}(\tau=0)=0$ for a reasonable range of Deborah numbers that are characteristic of soft and rigid biomaterials, as well as those that experience dielectric relaxation when $De\approx 1$. The amplitude of the electric potential difference across the capacitor plates V_0 represents a convenient parameter for systematic variation of the electric-field-sensitive intra-tissue Damköhler number, according to Eq. (15). The dimensionless parameter ξ that characterizes the weak-field dependence of intra-tissue diffusivities on E^2 is given by:

$$\begin{aligned}D_{A,effective,intra-tissue}&=D_{A,zero-field}\left\{1+\Omega E^2+\ldots\right\}\\&=D_{A,zero-field}\left\{1+\xi\Lambda^4_{A,electric}\sin^2(\omega t)+\ldots\right\}\end{aligned} \tag{24}$$

$$\xi=\Omega\left\{\frac{\rho_{nutrient,medium}}{\gamma_{electric}\varepsilon_0\{\varepsilon_S-\varepsilon_\infty\}\Theta_{Diffusion,zero-field}}\right\}^2$$

Time-averaging of E^2 was not employed in Eqs. (13), (19), and (24) because the period of oscillation of the electric potential (i.e., $2\pi/\omega$) is of the same order-of-magnitude as the time constant for diffusion under zero-field conditions, $\Theta_{Diffusion,zero\text{-}field}$. Rigorously, the effective intra-tissue diffusivity is a symmetric 2nd-rank tensor in which the electric potential only affects the diagonal elements, via Eqs. (10) and (24). Hence, Ω and ξ vanish when radial diffusion in Eq. (19) is analyzed with electric field vectors oriented in the z-direction. The initial rate of increase of δ_{MTBLT} with respect to τ is infinitely fast, according to the first term due to diffusion on the right side of Eq. (19) that does not depend on zero-field or electric-field-stimulated rates of consumption. Analogously, the diffusion terms are dominant on the right side of Eq. (7) [i.e., derivatives of $\rho_{nutrient}$ with respect to r] and Eq. (13) [i.e., derivatives of Ψ_A with respect to η] at $\tau=0$, prior to the development of the mass transfer boundary layer. Previous analytical solutions of the modified diffusion equation with simple nth-order kinetics (i.e., n = 0,1,2) in biomaterials with rectangular symmetry [28] reveal that $\delta_{MTBLT}\approx 0.0346$ at $\tau=10^{-4}$ when $\Lambda_{A,zero\text{-}field}=4$. This pseudo-initial condition is employed in this investigation. Biomaterial response is analyzed by capturing the time dependence of tissue-averaged dimensionless nutrient mass density, defined according to Eq. (25);

$$\begin{aligned}&\frac{1}{\rho_{nutrient,medium}\pi R^2_{circular}d}\int_{z=0}^{z=d}dz\int_{\theta=0}^{\theta=2\pi}d\theta\int_{r=r_{critical}}^{r=R_{circular}}\rho_{nutrient}(r,t)r\,dr\\&=2\int_{\eta=1-\delta_{MTBLT}}^{\eta=1}\Psi_A(\eta,\tau)\eta d\eta=2\delta_{MTBLT}(\tau)\int_{\varphi=0}^{\varphi=1}\left\{\alpha+\beta\varphi+\zeta\varphi^2\right\}\{1-\varphi\delta_{MTBLT}(\tau)\}d\varphi\\&=2\delta_{MTBLT}(\tau)\left\{\left(\alpha+\frac{1}{2}\beta+\frac{1}{3}\zeta\right)-\left(\frac{1}{2}\alpha+\frac{1}{3}\beta+\frac{1}{4}\zeta\right)\delta_{MTBLT}(\tau)\right\}\\&\underset{\beta=-2}{\alpha=\zeta=1}\frac{1}{6}\delta_{MTBLT}(\tau)\{4-\delta_{MTBLT}(\tau)\}\end{aligned} \tag{25}$$

Tissue-averaged dimensionless nutrient mass density, given by the function in Eq. (25), is illustrated in Fig. 3 when dielectric relaxation occurs in porous biomaterials, electric-field-enhanced intra-tissue diffusion is neglected, and the zero-field intra-tissue Damköhler number is greater than its critical value of 53 [see Eq. (23)], such that the tissue's inner core, defined by $0\le\eta\le 1-\delta_{MTBLT}$, is starved of the essential ingredients required for cell sustainability and proliferation.

One qualitatively identifies a *critical* electric-field-sensitive intra-tissue Damköhler number $\Lambda^2{}_{A,electric,critical}\approx 10$ to achieve at least 10% absolute decrease in tissue-averaged nutrient mass density relative to steady state zero-field conditions when $\Lambda^2{}_{A,zero\text{-}field}=100$ in Fig. 3.

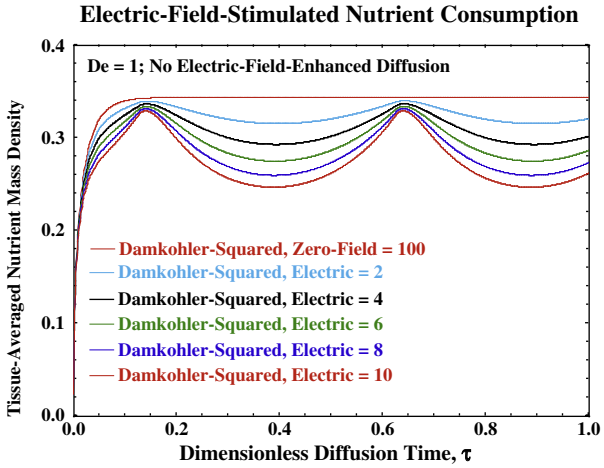

Fig. 3. von Kármán–Pohlhausen tissue-averaged dimensionless nutrient mass density, according to Eq. (25) via the solution of Eq. (19) for electric-field-stimulated nutrient consumption in porous biomaterials with cylindrical symmetry that experience dielectric relaxation (i.e., De = 1). Electric-field enhancement of intra-tissue diffusion is not considered. The zero-field intra-tissue Damköhler number (i.e., $\Lambda^2_{A,zero\text{-}field} = 100$) is greater than its critical value of 53, according to Eq. (23), when the initial conditions for cellular and oxygen mass densities on the external biomaterial surface are: Ψ_{cells} $(\eta = 1, \tau = 0) = 0.25$ and Ψ_{oxygen} $(\eta = 1, \tau = 0) = 1$. The effect of harmonic external electric potential on tissue-averaged nutrient mass density increases from the zero-field uppermost curve to the lowermost curve. The critical electric-field-sensitive intra-tissue Damköhler number is approximately 10% of the zero-field intra-tissue Damköhler number. Parameters: $\omega = 2\pi$ radians/s, $\Theta_{Diffusion,zero\text{-}field}/\lambda = 2\pi$, $\xi = 0$, 1000 steps in dimensionless diffusion time τ, from $\tau = 0$ to $\tau = 1$.

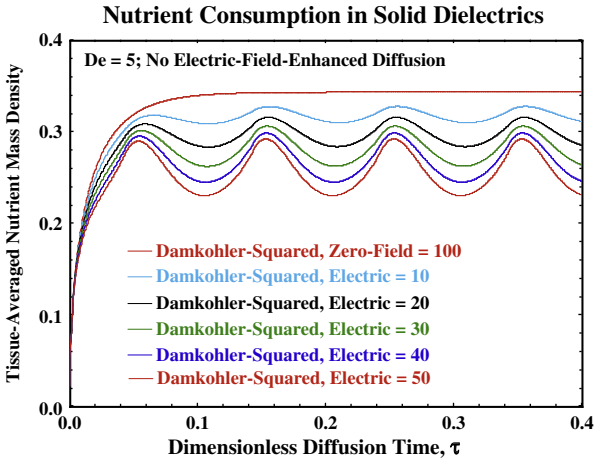

Fig. 4. von Kármán–Pohlhausen tissue-averaged dimensionless nutrient mass density, according to Eq. (25) via the solution of Eq. (19) for electric-field-stimulated nutrient consumption in rigid biomaterials (i.e., De = 5) with cylindrical symmetry. Electric-field enhancement of intra-tissue diffusion is not considered. The zero-field intra-tissue Damköhler number (i.e., $\Lambda^2_{A,zero\text{-}field} = 100$) is greater than its critical value of 53, according to Eq. (23), when the initial conditions for cellular and oxygen mass densities on the external biomaterial surface are: Ψ_{cells} $(\eta = 1, \tau = 0) = 0.25$ and Ψ_{oxygen} $(\eta = 1, \tau = 0) = 1$. The effect of harmonic external electric potential on tissue-averaged nutrient mass density increases from the zero-field uppermost curve to the lowermost curve. The critical electric-field-sensitive intra-tissue Damköhler number is approximately 40% of the zero-field intra-tissue Damköhler number. Parameters: $\omega = 2\pi$ radians/s, $\Theta_{Diffusion,zero\text{-}field}/\lambda = 2\pi$, $\xi = 0$, 1000 steps in dimensionless diffusion time τ, from $\tau = 0$ to $\tau = 0.4$.

Harmonic excitation of solid-like biomaterials at higher Deborah numbers in Fig. 4 occurs at the same frequency (i.e., 1 Hz.) relative to the simulations in Fig. 3 when De = 1, but the dimensional analysis of time in the harmonic electric potential includes the Deborah number [i.e., see Eq. (13)]. Hence, higher Deborah number response translates to higher perceived oscillation frequency for nutrient boundary layer thickness and tissue-averaged nutrient mass density on the dimensionless time axis when the ratio of the zero-field diffusion time constant $\Theta_{Diffusion,zero\text{-}field}$ to the material response time $\lambda(T)$ remains the same, even though each time constant is longer in rigid solids relative to those that undergo dielectric relaxation. The effect of the Deborah number on the real and imaginary components of the complex dielectric constant, according to Eq. (4), is primarily responsible for (i) smaller amplitude oscillatory response in Fig. 4 relative to Fig. 3, and (ii) the fact that larger electric-field-sensitive intra-tissue Damköhler numbers in rigid biomaterials are required to induce a significant decrease in the tissue-averaged nutrient mass density relative to zero-field simulations. For example, the *critical* electric-field-sensitive intra-tissue Damköhler number $\Lambda^2_{A,electric,critical} \approx 40$ in Fig. 4 to achieve at least 10% absolute decrease in tissue-averaged nutrient mass density relative to steady state zero-field conditions when $\Lambda^2_{A,zero\text{-}field} = 100$ and De = 5.

8. Conclusions

Biological systems respond to mechanical stress and electro-kinetic stimulation, via complex mechano-transduction [51,52] and electro-transduction pathways. In this research contribution, dynamic dielectric spectroscopy in viscoelastic polymers and the Debye equation with one relaxation time are employed to calculate induced dipole polarization in response to harmonic electric potential excitation. Nutrient consumption and cell proliferation are stimulated by induced dipole polarization in polymeric scaffolds that contain anchorage-dependent mammalian cells. A cylindrical geometry is analyzed with dielectric biomaterials sandwiched between a parallel-plate capacitor, such that the electric-field vectors are aligned with the z-direction. Due to the impermeable capacitor plate boundaries, nutrient media are exposed to these porous biomaterials along their circumference, allowing radial diffusion of nutrients and growth factors inward to support cell proliferation and sustainability. Important new concepts that do not appear elsewhere in the research literature are summarized by the following equations: Eq. (5) describes electro-kinetic rates of nutrient consumption, Eq. (13) represents the dimensionless reaction–diffusion equation that includes the Damköhler and Deborah numbers, Eq. (15) defines the electric-field-sensitive intra-tissue Damköhler number, Eq. (19) describes time-evolution of the nutrient boundary layer thickness, and Eq. (23) evaluates the critical value of the zero-field intra-tissue Damköhler number. Diffusional mass flux radially inward is essentially "uncoupled" from electric-field vectors in the z-direction, but the dielectric nature of polymeric biomaterials generates dipole polarization density that catalyzes enhanced rates of nutrient consumption and cell proliferation. It is desirable to develop regenerative tissue under reaction–diffusion conditions where the zero-field intra-tissue Damköhler number is less than its critical value to guarantee that the entire porous biomaterial matrix is exposed to nutrients, oxygen, and growth factors at steady state. The von Kármán–Pohlhausen integral method of boundary layer analysis of the reaction–diffusion equation reveals time-dependent growth of the mass transfer boundary layer inward from the external tissue/nutrient-medium interface toward the central core. Nutrient mass transfer boundary layer thickness δ_{MTBLT} appears as a time-dependent length scale in the denominator of the combined independent variable φ, via Eq. (16), and δ_{MTBLT} satisfies Eq. (19) for radial diffusion in dielectric biomaterials with anchorage-dependent cells that experience electric-field-stimulated nutrient consumption. The Damköhler and Deborah numbers provide a unique description of diffusion and electro-kinetic stimulation of nutrient consumption when viscoelastic relaxation occurs. The critical value of the electric-field-sensitive intra-tissue Damköhler number $\Lambda^2_{A,electric,critical}$, above which it is necessary to consider the effect of harmonic electric potential on nutrient consumption for tissue regeneration, is proportional to the Deborah number and corresponds to a larger

fraction of the zero-field intra-tissue Damköhler number in rigid dielectric biomaterials.

Acknowledgments

LA Belfiore gratefully acknowledges the Provincia Autonoma di Trento for research support during his extended sabbatical at the University of Trento. Professor Matt Kipper in the Department of Chemical and Biological Engineering at Colorado State University has been a source of inspirational support throughout all of these tissue-based bioreactor simulations. Michael Floren, a PhD student in the Department of Materials Engineering and Industrial Technologies at the University of Trento, is acknowledged for helpful discussions about cell proliferation in porous biomaterials.

References

[1] G. Marsh, H.W. Beams, In-vitro control of growing check nerve fibers by applied electric currents, Journal of Cellular and Comparative Physiology 27 (3) (1946) 139–157.
[2] B. Song, M. Zhao, J.V. Forrester, C.D. McCaig, Electrical cues regulate the orientation and frequency of cell division and the rate of wound healing in-vivo, Proceedings of the National Academy of Science 99 (21) (2002) 13577–13582.
[3] L.C. Kloth, Electrical stimulation for wound healing: a review of evidence from in-vitro studies, animal experiments, and clinical trials, Lower Extremity Wounds 4 (23) (2005) 23–44.
[4] R. Goodman, C.A.L. Bassett, A.S. Henderson, Pulsing electromagnetic fields induce cellular transcription, Science 220 (4603) (1983) 1283–1285.
[5] C.A.L. Bassett, I. Herrmann, Effect of electrostatic fields on macromolecular synthesis by fibroblasts in-vitro, The Journal of Cell Biology 39 (2P2) (1968) A9.
[6] G. Bourguignon, L. Bourguignon, Electric stimulation of protein and DNA synthesis in human fibroblasts, The FASEB Journal 1 (5) (1987) 398–402.
[7] C. Erickson, R. Nuccitelli, Embryonic fibroblast motility and orientation can be influenced by physiological electric fields, The Journal of Cell Biology 98 (1984) 296–307.
[8] C.A.L. Bassett, R.J. Pawluk, R.O. Becker, Effects of electric currents on bone in-vivo, Nature 204 (1964) 652–654.
[9] A.N. Zengo, C.A.L. Bassett, G. Prountzos, R.J. Pawluk, A.A. Pilla, In-vivo effects of direct current in mandible, Journal of Dental Research 55 (3) (1976) 383–390.
[10] D.D. Levy, B. Rubin, Inducing bone growth in-vivo by pulsed stimulation, Clinical Orthopaedics and Related Research 88 (1972) 218–222.
[11] C.A.L. Bassett, R.J. Pawluk, A.A. Pilla, Augmentation of bone repair by inductively coupled electromagnetic fields, Science 184 (4136) (1974) 575–577.
[12] L. Vodovnik, D. Miklavcic, G. Sersa, Modified cell proliferation due to electrical currents, Cellular Engineering: Medical & Biological Engineering & Computing 30 (4) (1992) 21–28.
[13] J.P. Busalmen, S.R. de Sánchez, Electrochemical polarization-induced changes in the growth of individual cells and biofilms of *Pseudomonas fluorescens*, Applied and Environmental Microbiology 71 (10) (2005) 6235–6240.
[14] M.T. Tsai, W.H.S. Chang, K. Chang, R.J. Hou, T.W. Wu, Pulsed electromagnetic fields affect osteoblast proliferation and differentiation in bone tissue engineering, Bioelectromagnetics 28 (2007) 519–528.
[15] N.G. Maroudas, Chemical and mechanical requirements for fibroblast adhesion, Nature 244 (1973) 353–354.
[16] J.H. Lee, J.W. Lee, G. Khang, H.B. Lee, Interaction of cells on chargeable-functional-group gradient surfaces, Biomaterials 18 (4) (1997) 351–358.
[17] A. Kishida, H. Iwata, Y. Tamada, Y. Ikada, Cell behavior on polymer surfaces grafted with non-ionic and ionic monomers, Biomaterials 12 (1991) 786–792.
[18] S.F. Rose, A.L. Lewis, G.W. Hanlon, A.W. Lloyd, Biological responses to cationically charged phosphorylcholine-based materials in-vitro, Biomaterials 25 (2004) 5125–5135.
[19] J.A. Spadaro, Mechanical and electrical interactions in bone remodeling, Bioelectromagnetics 18 (3) (1997) 193–202.
[20] K. Yonemori, S. Matsunaga, Y. Ishidou, S. Maeda, H. Yoshida, Early effects of electrical stimulation on osteogenesis, Bone 19 (2) (1996) 173–180.
[21] S. Bechara, L. Wadman, K.C. Popat, Electro-conductive polymeric nanowire templates facilitate in-vitro neural stem cell line adhesion, proliferation, and differentiation, Acta Biomaterialia 7 (7) (2011) 2892–2901.
[22] M.A. Matos, M.T. Cicerone, Alternating-current electric field effects on neural stem cell viability and differentiation, Biotechnology Progress 26 (2010) 664–670.
[23] L.D. Landau, E.M. Lifshitz, L.P. Pitaevskii, Electrodynamics of Continuous Media, Courses in Theoretical Physics, 2nd edition, Electrostatics of Dielectrics, Volume 8, Pergamon Press, 1984, Chapter 2.
[24] J.D. Jackson, Classical Electrodynamics, 2nd edition, Wiley, New York, 1975, p. 33, 34, 144–146, 210–213.
[25] K. John, D. Caillerie, P. Peyla, M. Ismail, A. Raoult, J. Prost, C. Misbah, Actin-based propulsion: intriguing interplay between material properties and growth processes, Ch.#2, in: A. Chauviere, L. Preziosi, C. Verdier (Eds.), Cell Mechanics: From Single Scale-Based Models to Multiscale Modeling, Chapman & Hall (CRC), Mathematical and Computational Biology Series, Taylor & Francis Group, Boca Raton, FLA, 2010, pp. 29–66.
[26] J. van Turnhout, Thermally stimulated discharge currents in polymeric electrets, Polymer Journal 2 (1971) 173–191.
[27] S.R. de Groot, P. Mazur, Nonequilibrium Thermodynamics, Dover, New York, 1984, pp. 143–148, Chap. 8.
[28] L.A. Belfiore, Physical Properties of Macromolecules, Wiley, Hoboken, NJ, 2010 Chaps. 4,10,15.
[29] R.L. Magin, Fractional calculus models of complex dynamics in biological tissues, Computers and Mathematics with Applications 59 (5) (2010) 1586–1593.
[30] P.M. Doran, Bioprocess Engineering, Academic Press, 1995, p. 276.
[31] S.J. Pirt, Principles of Microbe and Cell Cultivation, Blackwell Scientific, Oxford University Press, 1975.
[32] P. Pathi, T. Ma, B.R. Locke, Role of nutrient supply on cell growth in bioreactor design for tissue engineering of hematopoietic cells, Biotechnology and Bioengineering 89 (7) (2005) 743–758.
[33] J.E. Bailey, D.F. Ollis, Biochemical Engineering Fundamentals, 2nd ed. McGraw-Hill, New York, 1986.
[34] G.A. Truskey, F. Yuan, D.F. Katz, Transport Phenomena in Biological Systems, 2nd edition Prentice Hall, Upper Saddle River, NJ, 2009 Chaps. 10 & 12.
[35] B.A. Grzybowski, Chemistry in Motion: Reaction–diffusion Systems for Micro- and Nano-technology, Wiley, Hoboken, NJ, 2009.
[36] R. Baronas, F. Ivanauskas, J. Kulys, Mathematical Modeling of Biosensors: An Introduction for Chemists and Mathematicians, Springer, Heidelberg, 2010.
[37] L.A. Belfiore, M.L. Floren, F.Z. Volpato, A.T. Paulino, C.J. Belfiore, Nutrient diffusion and simple n^{th}-order consumption in regenerative tissue and biocatalytic sensors, Biophysical Chemistry 155 (2–3) (2011) 65–73.
[38] R.B. Bird, W.E. Stewart, E.N. Lightfoot, Transport Phenomena, 2nd edition Wiley, Hoboken, NJ, 2002 Chaps. 18,19.
[39] L.A. Belfiore, Transport Phenomena for Chemical Reactor Design, Wiley, Hoboken, NJ, 2003 Chaps. 10,15,16,21,25.
[40] M. Zakari, D. Jou, A generalized Einstein relation for flux-limited diffusion, Physica A 253 (1998) 205–210.
[41] P. Kleinert, V.V. Bryksin, Unified quantum approach for electric-field-dependent drift velocities and diffusion coefficients, Physics Letters A 317 (3–4) (2003) 315–323.
[42] V.V. Bryksin, P. Kleinert, Theory of quantum diffusion in biased semiconductors, Journal of Physics: Condensed Matter 15 (9) (2003) 1415–1425.
[43] J.W. Henshaw, D.A. Zaharoff, B.J. Mossop, F. Yuan, Electric-field-mediated transport of plasmid DNA in tumor interstitium in-vivo, Bioelectrochemistry 71 (2007) 233–242.
[44] L.A. Belfiore, M.L. Floren, A.T. Paulino, C.J. Belfiore, Stress-sensitive tissue regeneration in viscoelastic biomaterials subjected to modulated tensile strain, Biophysical Chemistry 158 (1) (2011) 1–8.
[45] T.R. Gowrishankar, J.C. Weaver, An approach to electrical modeling of single and multiple cells, Proceedings of the National Academy of Science 100 (6) (March 18th 2003) 3203–3208.
[46] T. Bandyopadhyay, S.K. Ghosh, M. Tachiya, Diffusion-influenced fluorescence quenching by electron transfer: effect of an external electric field, Israel Journal of Chemistry 44 (2004) 119–125.
[47] L. Debnath, Nonlinear Partial Differential Equations for Scientists & Engineers, Nonlinear Diffusion–Reaction Phenomena, 2nd edition, Birkhäuser, Boston, 2005 Chap. 8.
[48] M. Bendahmane, K.H. Karlsen, Analysis of a class of degenerate reaction–diffusion systems and the bidomain model of cardiac tissue, Networks and Heterogeneous Media, American Institute of Mathematical Sciences 1 (1) (March 2006) 185–218.
[49] J.A. Sherratt, S.A. Gourley, N.J. Armstrong, Bounded solutions of a non-local reaction–diffusion model for adhesion in cell aggregation and cancer invasion, European Journal of Applied Mathematics 20 (2009) 123–144.
[50] J. Prakash, G.P. Raja Sekhar, S. De, M. Böhm, A criterion to avoid starvation zones for convection–diffusion–reaction problems in porous biological pellets under oscillatory flow, International Journal of Engineering Science 48 (2010) 693–707.
[51] V. Barron, E. Lyons, C. Stenson-Cox, P.E. McHugh, A. Pandit, Bioreactors for cardiovascular cell and tissue growth: a review, Annals of Biomedical Engineering 31 (2003) 1017–1030.
[52] D.L. Bader, D.L. Lee, Mechanical conditioning of cell-seeded constructs for soft-tissue repair: are optimization strategies possible, in: J. Chaudhuri, M. Al-Rubeai (Eds.), Bioreactors for Tissue Engineering: Principles, Design & Operation, Springer, The Netherlands, 2005, pp. 165–192, Chapter 7.

Glossary

d: thickness of dielectric biomaterial, sandwiched between capacitor plates
D_{AB}*:* binary molecular diffusion coefficient
$D_{A,effective}$*:* intra-tissue diffusion coefficient for species A
$D_{A,zero\text{-}field}$*:* intra-tissue diffusion coefficient for species A under zero-field conditions
De: Deborah number; {material response time}/{time scale for deformation}
E: ac electric field
$k_{Boltzmann}$*:* Boltzmann's constant
$k_{zero\text{-}field}$*:* kinetic rate constant for 3rd-order pseudo-homogeneous rate of consumption under zero-field conditions; $\{volume/mass\}^2/time$
MW_i*:* molar mass of species *i*
P: dipole polarization density, Coulomb-cm/cm^3
r: spatial coordinate measured in the radial direction, cylindrical coordinates

$r_{critical}$: critical value of the spatial coordinate in the radial direction for cylindrical tissue, below which reactants do not penetrate the central core of the tissue
$R_{circular}$: radius of porous dielectric biomaterials with cylindrical symmetry
$R_{homogeneous}$: rate of pseudo-homogeneous nutrient consumption, with contributions from zero-field and electric-field-sensitive kinetic pathways; mass/{volume–time}
t: independent variable for transient response, time
T: absolute temperature
V: electric potential applied across capacitor plates
V_0: amplitude of the harmonic electric potential applied across capacitor plates
x_i: mole fraction of species i

Greek symbols

α,β,ζ: coefficients in the quadratic function for dimensionless nutrient mass density Ψ_A, see Eq. (16)
$\gamma_{electric}$: scalar electro-kinetic coupling coefficient, mass/{thickness–Coulomb–time}
δ_{MTBLT}: time-dependent dimensionless mass transfer boundary layer thickness
∇: gradient operator
$\varepsilon_{porosity}$: void volume fraction for porous biomaterials
ε_0: permittivity of free space, 8.854×10^{-12} C^2/(N-m^2)
ε_S: dielectric constant at zero-frequency
ε_∞: optical dielectric constant at very high frequency
$\varepsilon'(\omega)$: real part of the complex dielectric constant, electrical storage component
$\varepsilon''(\omega)$: imaginary part of the complex dielectric constant, dissipative component
ε^*: complex dielectric constant: $\varepsilon' - j\varepsilon''$
φ: combined variable in the von Kármán–Pohlhausen quadratic molar density profile, see Eq. (16)
κ: polarization coefficient, or dielectric susceptibility
κ_A: partial molar dielectric susceptibility of species A
λ (T): material response time for dielectric biomaterials
$\Lambda_{A,zero\text{-}field}$: intra-tissue Damköhler number, order-of-magnitude estimate of the rate of consumption with respect to the rate of species-specific diffusion toward the central tissue core, both rate processes occur under zero-field conditions
$\Lambda_{A,zero\text{-}field,critical}$: critical value of the zero-field intra-tissue Damköhler number, above which the tissue's central core is starved of essential nutrients at steady state
$\Lambda_{A,electric}$: electric-field-sensitive intra-tissue Damköhler number, order-of-magnitude estimate of the electric-field-enhanced rate of consumption with respect to the zero-field rate of species-specific diffusion toward the central tissue core
η: dimensionless spatial coordinate in the radial direction for tissue with cylindrical symmetry; Eq. (12)
μ_i: chemical potential of species i
υ_i: stoichiometric coefficients for reactants (i.e., oxygen) and products (i.e., cells)
ρ_{cells}: mass density of attached cells within porous biomaterials
$\rho_{nutrient}$: intra-tissue mass density of nutrients
$\rho_{nutrient,medium}$: mass density of nutrients on the external biomaterial surface, at $r = R_{circular}$
ρ_{oxygen}: intra-tissue mass density of dissolved oxygen
ξ: dimensionless coefficient that describes electric field enhancement of intra-tissue diffusivity, Eq. (24)
Ψ_A: dimensionless mass density of nutrients, defined in Eq. (12)
Ψ_{cells}: dimensionless mass density of attached cells
Ψ_{oxygen}: dimensionless mass density of dissolved oxygen
$\sigma_{cells}/\sigma_{nutrient}$: stoichiometric ratio of the mass of cells produced per mass of nutrients consumed, ≈ 0.45
$\sigma_{oxygen}/\sigma_{nutrient}$: stoichiometric ratio of the mass of oxygen consumed per mass of nutrients consumed, ≈ 1
$\Theta_{Diffusion,zero\text{-}field}$: characteristic time constant for intra-tissue diffusion under zero-field conditions; $R^2_{circular}/D_{A,zero\text{-}field}$
τ: dimensionless independent time variable, defined in Eq. (12)
$\tau_{tortuosity}$: tortuosity factor for porous biomaterials
ω: frequency of harmonic electric potential applied across capacitor plates
ω_A: mass fraction of species A
Ω: coefficient that describes electric field enhancement of intra-tissue diffusivity, Eq. (10)
χ: mobility, or inverse friction coefficient, for Einstein diffusivity, Eq. (10)